AGU PUBLICATIONS

Geochemistry, Geophysics, Geosystems

RESEARCH ARTICLE
10.1002/2013GC005053

**Key Points:**
- Rare mafic to felsic plutonic suites were found at two Mariana fore-arc sites
- Suites are chemically like the boninite magma formed at subduction initiation
- Earliest stages of arc crust development can form intermediate to felsic plutons

**Supporting Information:**
- README
- Table S1

**Correspondence to:**
J. A. Johnson,
jjohn013@fiu.edu

**Citation:**
Johnson, J. A., R. Hickey-Vargas, P. Fryer, V. Salters, and M. K. Reagan (2014), Geochemical and isotopic study of a plutonic suite and related early volcanic sequences in the southern Mariana forearc, *Geochem. Geophys. Geosyst.*, *15*, 589–604, doi: 10.1002/2013GC005053.

Received 23 SEP 2013
Accepted 20 JAN 2014
Accepted article online 27 JAN 2014
Published online 17 MAR 2014

# Geochemical and isotopic study of a plutonic suite and related early volcanic sequences in the southern Mariana forearc

**Julie A. Johnson[1], Rosemary Hickey-Vargas[1], Patricia Fryer[2], Vincent Salters[3], and Mark K. Reagan[4]**

[1]Department of Earth and Environment, Florida International University, Miami, Florida, USA, [2]Hawai'i Institute of Geophysics and Planetology, University of Hawai'i, Honolulu, Hawai'i, USA, [3]National High Magnetic Field Laboratory, Florida State University, Tallahassee, Florida, USA, [4]Department of Geoscience, University of Iowa, Iowa City, Iowa, USA

**Abstract** The forearc of the southern Mariana arc preserves igneous suites formed during the initiation of subduction between the Pacific and Philippine Sea plates about 50 Ma ago. We have studied rare suites of gabbroic to tonalitic plutonic rocks dredged from two locations in the Mariana forearc by cruise by University of Hawai'i cruise KK81-06-26. Comparison of the chemical and isotopic (Sr, Nd, Pb, and Hf) characteristics of these rocks with well-studied volcanics from the forearc reveals that the plutonics from dredge RD63 and RD64 are chemically related to boninites erupted at 48–43 Ma. This is the first report of boninite-like plutonics in the southern Mariana trench. These suites have trace element characteristics consistent with island arc settings (U/Th: 0.58–1.44, Nb/La: 0.18–0.79) and other features uniquely connected with boninites: $TiO_2 < 0.15$ wt % and $Zr/Sm > 25$. RD63 plutonics resemble nearby boninite volcanics and were likely derived from differentiated boninite magma with 58% $SiO_2$, forming gabbro by crystal accumulation, diorite and quartz diorite by crystallization, and tonalite by crystallization and/or partial melting. The RD64 suite (gabbro through tonalite) may have had a more depleted magma source and formed by accumulation and crystallization only. Although the physical dimensions of the plutonic body are unknown, the relationship with boninites indicates that felsic intrusives can form during early stages of island arc development. Such rocks could form part of midcrustal low-velocity layers detected in arc crust by seismic studies. Tonalites similar to those studied here are also found in some ophiolites.

## 1. Introduction

The volcanic history of the southern Izu-Bonin-Mariana (IBM) arc system (Figure 1), starting with subduction initiation, has been relatively well characterized based on rocks recovered from dredge and submersible dive sampling and deep ocean drilling conducted by DSDP, ODP, IODP, JAMSTEC, and other US NSF funded cruises. Volcanic rocks in the Mariana forearc, including the fore-arc islands (e.g., Guam, Saipan, Rota) have been studied and described by *Bloomer* [1983], *Bloomer and Hawkins* [1987], *Hickey-Vargas* [1989], *Hickey-Vargas and Reagan* [1987], *Hickey and Frey* [1982], *Meijer* [1980], *Natland and Tarney* [1981], *Ohara et al.* [2008], *Pearce et al.* [1992], *Reagan and Meijer* [1984], and *Reagan et al.* [2008, 2013, 2010]. According to *Reagan et al.* [2010], the early volcanic sequence subsequent to subduction initiation was: (1) FABs or fore-arc basalts; then (2) boninites; then (3) volcanic rocks of typical island arc tholeiitic and calc-alkaline characteristics, as plate subsidence transitioned to true subduction [*Stern*, 2004; *Stern and Bloomer*, 1992]. Based primarily on K-Ar and Ar-Ar (and more recently U-Pb) radiogenic dating, the earliest volcanic activity in the IBM began 48–52 Ma [*Cosca et al.*, 1998; *Ishizuka et al.*, 2011, 2006; *Meijer et al.*, 1983; *Reagan et al.*, 2013] which approximately coincides with the proposed change in motion of the Pacific plate [*Clague and Dalrymple*, 1987; *Sharp and Clague*, 2006]. Thus, the early arc volcanic sequence in the IBM forearc records the process of subduction initiation and onset of arc magmatism [*Stern*, 2004; *Stern and Bloomer*, 1992].

In contrast to studies of volcanic rocks, few geochemical studies of the rare plutonic samples from this area have been conducted. Since the late 1970s, dredging of the trench wall in this region has yielded mafic to felsic plutonic rocks with poorly understood relationships to the volcanics [*Bloomer*, 1983; *Bloomer and Hawkins*, 1987]. Intermediate and felsic plutonics have also been recovered in other areas of the arc system, for example, in the northern Kyushu-Palau Ridge [*Haraguchi et al.*, 2003]. Such rocks may be representative of the middle crustal layer that has been inferred for much of the Izu-Bonin-Mariana arc crust from seismic *P* wave velocity studies [*Hacker et al.*, 2003; *Suyehiro et al.*, 1996; *Takahashi et al.*, 1998, 2008].

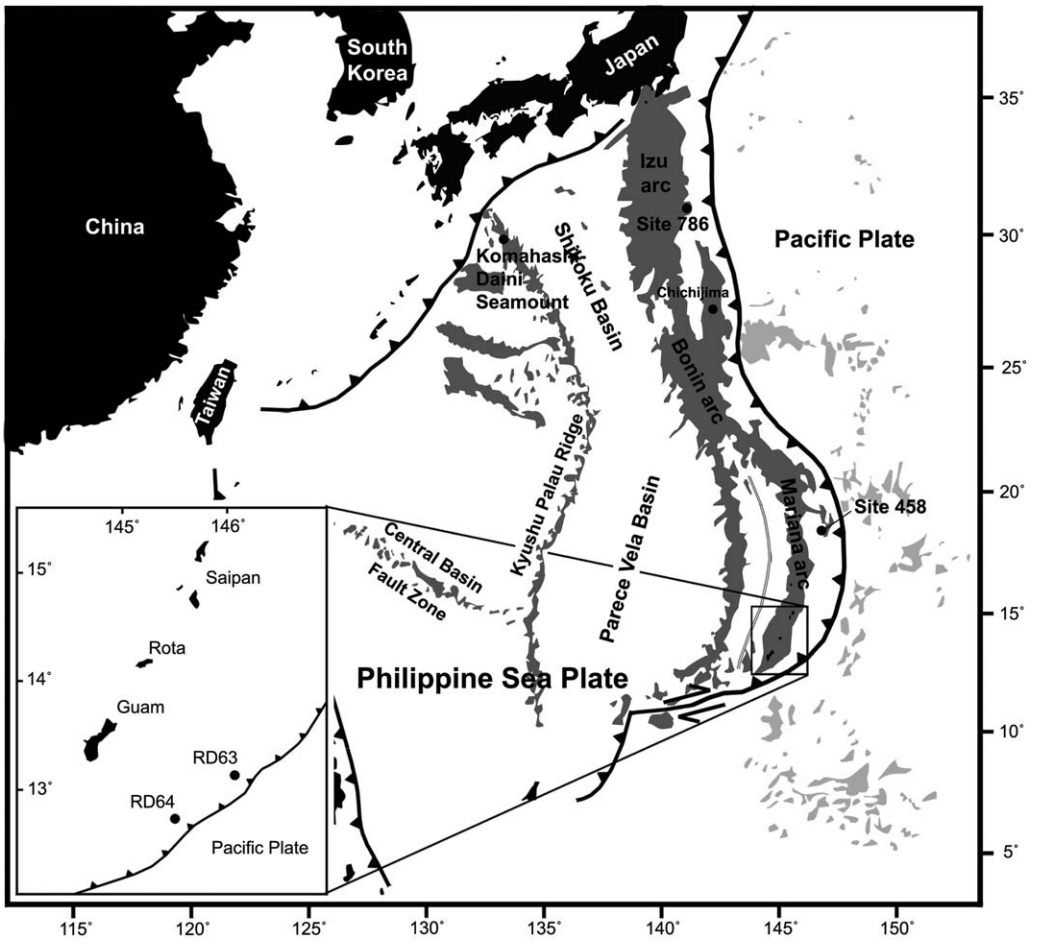


**Figure 1.** Location map of the Izu-Bonin-Mariana arc system. Inset showing locations of RD63 and RD64 collected by dredge during the 1981 cruise R/V Kana Keoki (KK) 81-06-26 by University of Hawai'i.

In this paper, we report and interpret geochemical data for plutonic rocks from two dredge sites on the inner Mariana Trench slope near Guam (Figure 1). These were recovered by the 1981 cruise of the University of Hawai'i R/V Kana Keoki, at Site RD63, at a depth of 8150–7420 m and RD64 at 7390–7195 m (Figure 1). Dredge RD63 was taken from a serpentine mud volcano and RD64 was taken 74 km to the southwest from a fault scarp. The bulk of the volume of both dredge hauls consisted of serpentinized peridotitic rock, mainly harzburgite. About 10% of the dredge hauls consisted of the plutonic samples used in this study, ranging from mafic to felsic in both RD63 and RD64, in addition to some hypabyssal rocks of intermediate composition at RD64. Data are interpreted in the context of the well-understood volcanic sequences.

## 2. Geologic Background of the Southern IBM

Figure 1 shows a location map of the IBM system and an inset of the southern Mariana forearc with the locations of dredges RD63 and RD64. *Reagan et al*. [2013] (in Figure 2) include a sketch map of the southern Mariana forearc that shows the crustal succession in this area. It also shows the location of a gabbro layer that is near the fault scarp from which RD64 is likely recovered, and includes the location of the serpentine mud volcano from which RD63 was recovered. FABs (or fore-arc basalts) were the first lavas to be erupted following the initiation of subduction of the Pacific plate beneath the Philippine Sea plate or its predecessor at 51–52 Ma [*Reagan et al*., 2010]. An extensional regime is inferred for this early stage of plate subsidence

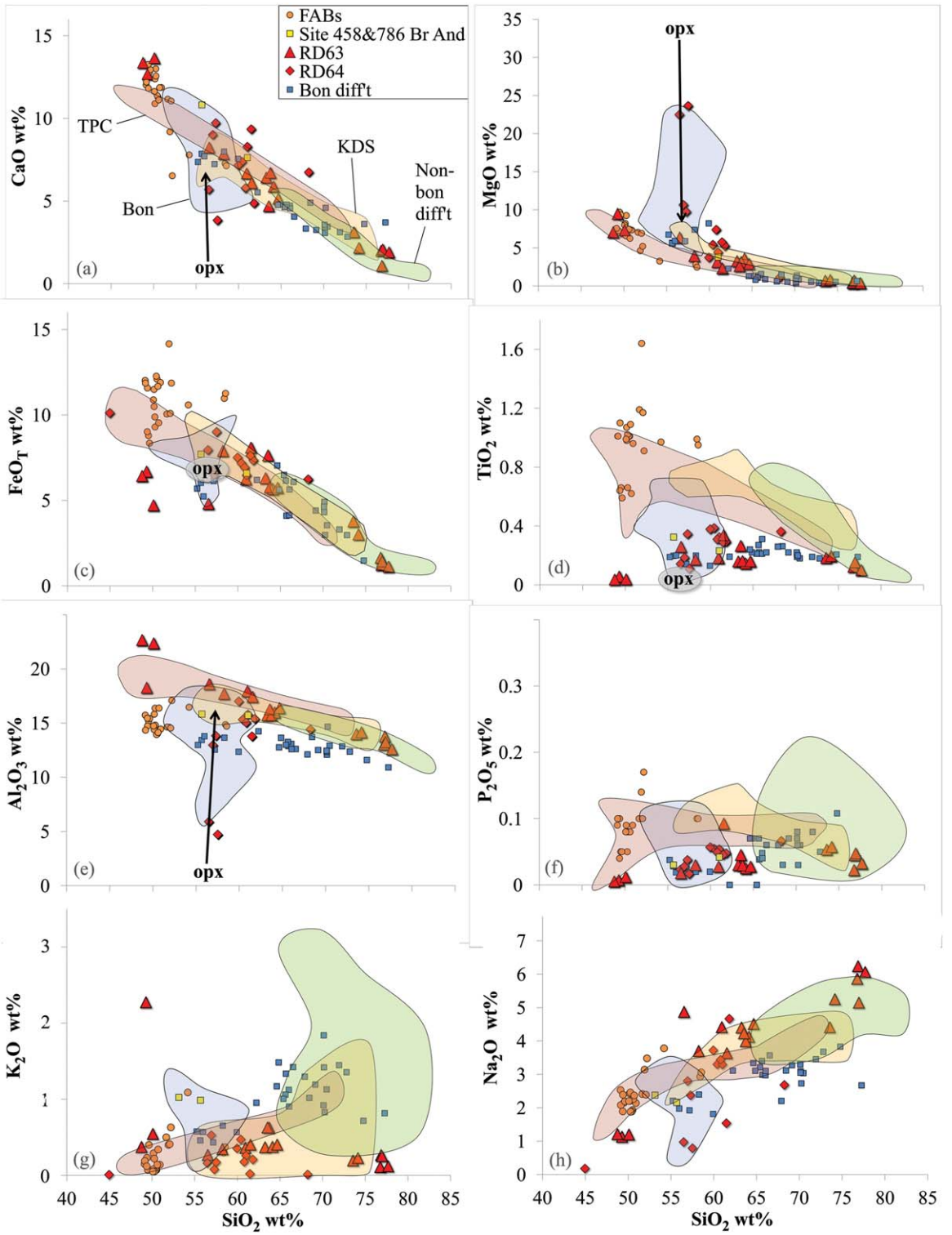


**Figure 2.** Major element data plotted versus $SiO_2$ wt %. Data points are rocks from RD63 and RD64 (red triangles and squares, this work), FABs (orange circles: *Reagan et al.* [2010]), and boninite differentiates (blue and yellow square symbols) such as andesites, dacites, and rhyolites from Chichijima [*Kuroda et al.*, 1988; *Taylor et al.*, 1994] and bronzite andesites from DSDP Sites 458 and 786 [*Pearce et al.*, 1999]. The blue field is boninites from Guam, the southern Mariana forearc and Chichijima ("Bon") [*Hickey-Vargas and Reagan*, 1987; *Pearce et al.*, 1999; *Reagan et al.*, 2010; *Taylor et al.*, 1994]. The red field is gabbro through tonalite from the Tanzawa Plutonic Complex ("TPC") in Honshu, Japan [*Kawate and Arima*, 1998]. The orange field is gabbro through tonalite from the Komahashi-Daini Seamount ("KDS") in the northern Kyushu-Palau Ridge [*Haraguchi et al.*, 2003]. The green field is for nonboninite related rhyolites from Saipan [*Reagan et al.*, 2008] and from Quaternary northern IBM volcanic centers [*Tamura et al.*, 2009] ("Non-bon diff't"). $FeO_T$ is total Fe. The orthopyroxene (OPX) data are from boninites analyzed by *Bloomer and Hawkins* [1987] and the arrows are an approximate fractionation trajectory.

and arc magmatism, with upwelling of asthenospheric mantle along fractures generated within the overriding plate lithosphere.

FABs have geochemical characteristics similar to depleted MORBs, but with varying extents of LIL (large ion lithophile) element enrichment caused by the addition of fluids from the subsiding Pacific lithosphere. Following FABs, boninites erupted in the same extensional environment. Boninites are generated by shallow hydrous melting of extremely depleted peridotite and require water from the subsiding lithosphere of the Pacific plate and high heat flux from the strongly upwelling upper mantle [*Bénard and Ionov*, 2012; *Bloomer and Hawkins*, 1987; *Hickey-Vargas and Reagan*, 1987; *Hickey and Frey*, 1982; *Ishizuka et al*., 2006; *Meijer*, 1980; *Meijer et al*., 1983; *Natland and Tarney*, 1981; *Pearce et al*., 1999; *Reagan and Meijer*, 1984]. These series are in the lower section of volcanic rocks in the forearc and constitute the IBM proto-arc [*Bloomer et al*., 1995; *Pearce et al*., 1999, 1992]. The uppermost section of volcanics in the forearc consists of "normal" tholeiitic and calc-alkaline volcanic rocks, marking the onset of true subduction and these are the volcanic products of the early IBM arc also called the first arc [*Gill*, 1981; *Gill et al*., 1994; *Meijer et al*., 1983]. A midcrustal layer of gabbros through tonalites is inferred from rare dredge and submersible samples of plutonic rocks on the trench wall. The existence of such a layer, and its thickness beneath the arc, is consistent with seismic cross sections of the northern and southern IBM [*Suyehiro et al*., 1996; *Takahashi et al*., 2008] which show a low *P* wave velocity layer in the middle crust. According to *Suyehiro et al*. [1996] and *Takahashi et al*. [2008], the low *P* wave velocity layer is consistent with lithologies including gabbros, diorites, plagiogranites, and tonalites based on density calculations.

## 3. Petrology

Igneous rock samples used for this study from KK81-06-26 dredge RD63 were 4–17 cm in size along the longest axis, and are categorized as tonalites, diorites, quartz diorites, and quartz gabbros based on normative mineralogy and by plotting them on a QAPF diagram. Petrographic examination of the RD63 suite shows varying amounts of quartz, plagioclase feldspar, orthopyroxene, clinopyroxene, hornblende, phyllosilicates (mainly chlorite), and magnetite. The composition of the ferromagnesian minerals depends in part on the degree of low grade alteration of the sample. Some samples have retained some primary pyroxene and hornblende while other samples display replacement by secondary amphiboles and phyllosilicates. Almost all plagioclase show signs of sericitization, although Ab contents increase with bulk rock $SiO_2$, consistent with igneous characteristics. Maximum grain sizes are 4.5 mm in gabbros, 1.8 mm in diorites, and 1.1–1.6 mm in tonalites.

Intrusive igneous rocks from KK81-06-26 dredge RD64 are mostly coarse-grained rocks: diorite, quartz diorite, and tonalite, with small amounts of diabase and bronzite andesite. Petrographic analyses show primarily quartz, plagioclase feldspar, orthopyroxene, clinopyroxene, hornblende, phyllosilicates (chlorite), and magnetite. The diabase and bronzite andesites contain chromite rather than magnetite. Grain sizes in RD64 rocks vary but are on the same scale as rocks from RD63, with the maximum grain sizes of $\sim$2 mm in plutonic rocks and 10–100 microns for minerals in the groundmass of the diabase and hypabyssal samples (phenocrysts in the bronzite andesites are 600 microns and the glomerocrysts are 2–3 mm in width). Zircons were observed in diorites, quartz diorites, and tonalites on microprobe backscatter images but they were $<$10 microns and at this time could not be dated.

## 4. Analytical Methods

Bulk analyses for representative rocks from RD63 and RD64 are given in Tables 1 and 2 and additional data are given in supporting information. Whole rock powders were prepared at Florida International University using an alumina ball-mill after cutting away alteration rinds and secondary veins and infilled fractures. Powders were sent to Washington State University (WSU) GeoAnalytical Lab in Pullman, WA for major and trace element analysis. Major elements were analyzed on a ThermoARL XRF with USGS BHVO-2 and two duplicate samples run to check analytical accuracy and precision (Table 1). The WSU Lab fused the sample powders into a low-dilution Li-tetraborate bead for X-ray fluorescence (XRF) analysis by methods described by *Johnson et al*. [1999]. Trace elements were analyzed on an Agilent 7700 inductively coupled plasma-mass spectrometry (ICP-MS) after fusion with di-lithium tetraborate, crushing, and dissolution with $HNO_3$-HF-$HClO_4$. Instrument drift was corrected using Ru, In, and Re as internal standards. More detailed

**Table 1.** Major and Trace Element Data for Representative Samples From KK81-06-26 RD63 and RD64 (The Complete Table 1, With 30 Samples, is Available as Supporting Information)

| Norm Lith[a] | USGS | Gbr | QDior | Dior | Ton | Br And | QDior | Dior | Alt Dior | Ton |
|---|---|---|---|---|---|---|---|---|---|---|
| Dredge | Std | RD63 | RD63 | RD63 | RD63 | RD64 | RD64 | RD64 | RD64 | RD64 |
| Sample | BHVO-2 | J22[b] | J27 | J29 | J46 | J49 | J53 | J61 | J63 | J65 |
| *Measured by XRF (wt %)* | | | | | | | | | | |
| $SiO_2$ | 50.18 | 49.32 | 60.29 | 57.74 | 77.10 | 55.56 | 58.70 | 55.41 | 55.10 | 66.67 |
| $TiO_2$ | 2.772 | 0.038 | 0.181 | 0.171 | 0.099 | 0.335 | 0.376 | 0.179 | 0.106 | 0.354 |
| $Al_2O_3$ | 13.76 | 22.02 | 17.75 | 17.56 | 12.50 | 13.42 | 14.89 | 12.62 | 4.52 | 14.09 |
| $FeO_T$[c] | 10.99 | 4.65 | 6.18 | 7.83 | 1.12 | 6.25 | 6.98 | 6.59 | 8.63 | 6.10 |
| MnO | 0.173 | 0.090 | 0.076 | 0.130 | 0.025 | 0.116 | 0.083 | 0.110 | 0.179 | 0.086 |
| MgO | 7.25 | 7.18 | 3.10 | 3.89 | 0.34 | 9.45 | 5.26 | 10.36 | 22.65 | 1.12 |
| CaO | 11.51 | 13.44 | 6.61 | 7.78 | 1.89 | 9.43 | 7.17 | 8.77 | 3.68 | 6.59 |
| $Na_2O$ | 2.24 | 1.18 | 4.37 | 3.67 | 6.02 | 2.31 | 3.21 | 2.73 | 0.76 | 2.62 |
| $K_2O$ | 0.52 | 0.54 | 0.36 | 0.34 | 0.12 | 0.08 | 0.46 | 0.51 | 0.17 | 0.01 |
| $P_2O_5$ | 0.267 | 0.012 | 0.027 | 0.030 | 0.032 | 0.037 | 0.053 | 0.027 | 0.016 | 0.065 |
| Sum | 99.66 | 98.46 | 98.93 | 99.15 | 99.25 | 96.99 | 97.18 | 97.31 | 95.82 | 97.70 |
| LOI | | 1.918 | 19.503 | 0.959 | 1.015 | 2.583 | 2.594 | 2.529 | 3.764 | 1.466 |
| *Measured by ICP-MS (ppm)* | | | | | | | | | | |
| Cs | 0.12 | 0.06 | 0.15 | 0.12 | 0.05 | 0.01 | 0.04 | 0.09 | 0.16 | 0.02 |
| Rb | 23.0 | 10.8 | 6.3 | 4.3 | 1.3 | 0.5 | 2.9 | 4.0 | 3.2 | 0.2 |
| Ba | 163 | 33 | 36 | 41 | 23 | 8 | 17 | 22 | 6 | 2 |
| Sr | 156 | 173 | 215 | 144 | 86 | 113 | 173 | 172 | 37 | 198 |
| Pb | 1.36 | 0.40 | 0.53 | 1.04 | 0.37 | 0.46 | 0.34 | 0.26 | 0.33 | 1.29 |
| Th | 1.10 | 0.05 | 0.25 | 0.27 | 0.44 | 0.14 | 0.24 | 0.16 | 0.06 | 0.35 |
| U | 0.47 | 0.05 | 0.33 | 0.32 | 0.60 | 0.09 | 0.18 | 0.11 | 0.06 | 0.30 |
| Nb | 1.40 | 0.09 | 0.64 | 0.56 | 0.97 | 0.35 | 0.51 | 0.31 | 0.16 | 0.67 |
| Ta | 0.12 | 0.01 | 0.06 | 0.06 | 0.12 | 0.02 | 0.04 | 0.02 | 0.01 | 0.05 |
| La | 5.67 | 0.37 | 2.05 | 2.29 | 1.26 | 1.38 | 2.16 | 1.50 | 0.62 | 3.43 |
| Ce | 12.15 | 0.66 | 3.68 | 4.41 | 2.20 | 3.83 | 5.74 | 3.91 | 1.46 | 8.25 |
| Pr | 1.52 | 0.09 | 0.54 | 0.64 | 0.34 | 0.61 | 0.93 | 0.60 | 0.23 | 1.27 |
| Nd | 6.01 | 0.39 | 2.30 | 2.78 | 1.58 | 3.09 | 4.45 | 2.93 | 1.07 | 6.00 |
| Zr | 84 | 5 | 43 | 51 | 94 | 27 | 46 | 28 | 12 | 68 |
| Hf | 2.57 | 0.15 | 1.25 | 1.53 | 2.73 | 0.79 | 1.37 | 0.87 | 0.38 | 2.00 |
| Sm | 1.43 | 0.11 | 0.60 | 0.81 | 0.47 | 1.07 | 1.38 | 0.97 | 0.35 | 1.80 |
| Eu | 0.44 | 0.07 | 0.24 | 0.24 | 0.30 | 0.40 | 0.46 | 0.38 | 0.12 | 0.58 |
| Gd | 1.49 | 0.13 | 0.70 | 0.95 | 0.57 | 1.44 | 1.66 | 1.30 | 0.44 | 2.18 |
| Tb | 0.26 | 0.02 | 0.13 | 0.17 | 0.10 | 0.27 | 0.30 | 0.24 | 0.08 | 0.38 |
| Dy | 1.74 | 0.17 | 0.81 | 1.16 | 0.72 | 1.88 | 1.96 | 1.61 | 0.55 | 2.47 |
| Ho | 0.39 | 0.04 | 0.18 | 0.27 | 0.17 | 0.41 | 0.42 | 0.35 | 0.12 | 0.54 |
| Er | 1.14 | 0.12 | 0.58 | 0.80 | 0.56 | 1.20 | 1.20 | 0.98 | 0.36 | 1.55 |
| Tm | 0.18 | 0.02 | 0.10 | 0.14 | 0.10 | 0.18 | 0.18 | 0.15 | 0.06 | 0.24 |
| Yb | 1.31 | 0.14 | 0.70 | 1.00 | 0.81 | 1.10 | 1.16 | 0.94 | 0.39 | 1.53 |
| Lu | 0.23 | 0.03 | 0.13 | 0.18 | 0.16 | 0.19 | 0.19 | 0.15 | 0.07 | 0.25 |
| Y | 10.68 | 0.97 | 5.33 | 6.94 | 4.99 | 10.26 | 10.84 | 8.81 | 3.15 | 14.13 |
| Sc | 8.1 | 33.7 | 24.9 | 36.8 | 11.7 | 33.1 | 28.8 | 36.4 | 28.0 | 20.5 |
| *Measured by XRF (ppm)* | | | | | | | | | | |
| Ni | 114 | 102 | 34 | 36 | 8 | 85 | 39 | 166 | 228 | 2 |
| Cr | 277 | 47 | 6 | 16 | 3 | 414 | 43 | 623 | 1697 | 2 |
| V | 311 | 104 | 200 | 241 | 32 | 195 | 273 | 159 | 102 | 113 |
| Zr | 167 | 6 | 44 | 52 | 92 | 28 | 46 | 29 | 12 | 66 |
| Ga | 21 | 14 | 14 | 13 | 11 | 9 | 16 | 11 | 5 | 15 |
| Cu | 134 | 19 | 26 | 12 | 8 | 2 | 3 | 11 | 45 | 5 |
| Zn | 104 | 25 | 24 | 40 | 4 | 33 | 23 | 35 | 52 | 25 |

[a]Normative lithologies, abbreviations: Gbr (Gabbro), Dior (Diorite), QDior (Quartz diorite), Alt Dior (Altered diorite), Br And (Bronzite andesite), and Ton (Tonalite).
[b]Values reported as an average from duplicate analyses. Standard deviation for all values is <3.0.
[c]$FeO_T$ as total Fe.

information about the standardization and correction factors can be found in the Technical Notes section of the WSU GeoAnalytical website.

Samples were chosen for Sr, Nd, Hf, and Pb isotope analysis based on major and trace element results, and they are all plutonic rocks. Given the extent and kind of alteration of the samples, powders were leached with 6 *N* HCl using a methodology based on *Mahoney* [1987] and *Weis and Frey* [1991, 1996] for ocean floor rocks. The leached powders were digested, processed, and analyzed at the Geochemistry Division of the National High Magnetic Field Laboratory (NHMFL) at Florida State University, Tallahassee, FL, using techniques reported in *Münker et al.* [2001], isotope separations were performed based on accepted techniques

**Table 2.** Isotopic Composition of Select Samples (Present-Day Values)[a]

| Sample | $^{87}Sr/^{86}Sr$ | $\pm 2\sigma$ | $^{143}Nd/^{144}Nd$ | $\pm 1\sigma$ | $^{176}Hf/^{177}Hf$ | $\pm 1\sigma$ | $^{206}Pb/^{204}Pb$ | $^{207}Pb/^{204}Pb$ | $^{208}Pb/^{204}Pb$ | $\varepsilon Nd_o$ | $\varepsilon Hf_o$ |
|---|---|---|---|---|---|---|---|---|---|---|---|
| RD63-J15 | 0.704029 | 0.000007 | 0.512943 | 0.000006 | 0.283050 | 0.000044 | 18.9400 | 15.5612 | 38.4452 | 5.90 | 9.84 |
| RD63-J23 | 0.704074 | 0.000008 | 0.512942 | 0.000005 | 0.283115 | 0.000004 | 18.9677 | 15.5536 | 38.4301 | 5.89 | 12.13 |
| RD63-J28 | 0.704219 | 0.000007 | 0.512961 | 0.000006 | 0.283174 | 0.000009 | 19.0648 | 15.5649 | 38.4711 | 6.26 | 14.23 |
| RD63-J29 | 0.703890 | 0.000007 | 0.512962 | 0.000005 | 0.283106 | 0.000003 | 19.0111 | 15.5596 | 38.4335 | 6.28 | 11.81 |
| RD63-J32 | 0.704253 | 0.000007 | 0.512947 | 0.000005 | 0.283123 | 0.000003 | 18.9928 | 15.5559 | 38.4134 | 5.99 | 12.41 |
| RD63-J34 | 0.703903 | 0.000008 | 0.512957 | 0.000004 | 0.283110 | 0.000004 | 18.9594 | 15.5493 | 38.3911 | 6.19 | 11.96 |
| RD63-J40 | 0.704330 | 0.000007 | 0.512960 | 0.000007 | 0.283099 | 0.000004 | 19.7930 | 15.6000 | 38.5797 | 6.24 | 11.55 |
| RD63-J45 | 0.704197 | 0.000007 | 0.512917 | 0.000005 | 0.283089 | 0.000004 | 19.4053 | 15.5797 | 38.4545 | 5.41 | 11.22 |
| RD64-J55 | 0.703666 | 0.000007 | 0.513050 | 0.000007 | 0.283164 | 0.000005 | 19.1504 | 15.5145 | 38.3734 | 8.00 | 13.86 |
| RD64-J58 | 0.703979 | 0.000011 | 0.513057 | 0.000006 | 0.283154 | 0.000003 | 18.9907 | 15.5011 | 38.2362 | 8.13 | 13.50 |
| RD64-J64 | 0.703614 | 0.000007 | 0.513044 | 0.000005 | 0.283130 | 0.000002 | 18.9077 | 15.4992 | 38.2375 | 7.88 | 12.67 |
| RD64-J65 | 0.703847 | 0.000007 | 0.513043 | 0.000005 | 0.283140 | 0.000002 | 18.9193 | 15.4990 | 38.2428 | 7.86 | 13.02 |

[a]Sr ratios measured on TIMS, standard E&A: ($^{87}Sr/^{86}Sr = 0.70808$); Nd, Hf, Pb ratios measured on Neptune ICPMS; Nd standard La Jolla: ($^{143}Nd/^{144}Nd = 0.511850$); Hf standard JMC475: ($^{176}Hf/^{177}Hf = 0.282000$); Pb standard NBS-981: ($^{206}Pb/^{204}Pb = 16.9356$; $^{207}Pb/^{204}Pb = 15.4891$; $^{208}Pb/^{204}Pb = 36.7006$) [*Todt et al.*, 1996]; $\varepsilon$Hf values calculated using the CHUR value (0.282772) established in *Blichert-Toft and Albarède* [1997].

[*Hart and Brooks*, 1977; *Manhès et al.*, 1978; *Richard et al.*, 1976; *Zindler et al.*, 1979] and modified by staff at NHMFL and *Salters* [1994] and *Salters et al.* [2011]. Sr isotopes were loaded on tungsten filaments and run on a Finnigan MAT TIMS, series 262. The $2\sigma$ values are reported in Table 2 and were corrected using repeated analysis of the E&A standard ($^{87}Sr/^{86}Sr = 0.70808$). Nd, Hf, and Pb isotopes were analyzed on a Finnigan Neptune MC-ICP-MS and $1\sigma$ values are reported. The synthetic La Jolla standard ($^{143}Nd/^{144}Nd = 0.511850$) was run with samples and the $1\sigma$ values were 0.000003. The JMC475 standard with $^{178}Hf/^{176}Hf = 0.28216$ was run with samples and the $1\sigma$ values were 0.000005 or less. $\varepsilon$Hf values are calculated using the chrondritic reservoir (CHUR) value (0.282772) established in *Blichert-Toft and Albarède* [1997] and are consistent with older literature. The Pb isotopes are corrected based on the accepted NBS-981 standard values ($^{206}Pb/^{204}Pb = 16.9356$; $^{207}Pb/^{204}Pb = 15.4891$; $^{208}Pb/^{204}Pb = 36.7006$) [*Todt et al.*, 1996]. A Tl spike was added to the samples for a Pb/Tl of ~6 and a $^{203}Tl/^{205}Tl$ standard (0.4188) was run with the samples as a correction for mass fractionation. Long-term averages of NBS-981 at NHMFL are $^{206}Pb/^{204}Pb = 16.9294 \pm 136$ ppm, $^{207}Pb/^{204}Pb = 15.4824 \pm 164$ ppm, and $^{208}Pb/^{204}Pb = 36.6698 \pm 211$ ppm based on numerous replications.

## 5. Geochemical Results

Eighteen samples from RD63 and 11 samples from RD64 were analyzed for major and trace elements, and 12 representative samples were analyzed for Sr, Nd, Hf, and Pb isotopes. Data from Tables 1 and 2, and supporting information, are plotted in Figures 2–7.

### 5.1. Major Elements

The major element compositions of the dredge site plutonic suites are compared to those of igneous rocks from other locations in the IBM forearc and southern Japan (Figure 2). The RD63 plutonic suite has $SiO_2$ of 49–78 wt %, MgO between 1 and 13 wt %, $Al_2O_3$ 13–23 wt %, $TiO_2 < 0.3$ wt %, and $K_2O$ of 0.11–2.3 wt %. The RD64 suite has $SiO_2$ of 56–68 wt %, MgO between 1 and 24 wt %, $Al_2O_3$ 4 and 17%, $TiO_2$ between 0.1 and 0.4 wt %, $K_2O$ of 0.01–0.53 wt %.

One notable major element characteristic of the rocks from RD63 is their extremely low $TiO_2$ contents (Figure 2d). RD64 rocks are slightly higher but still low compared with FABs, typical IBM arc lavas and mid-ocean ridge basalts (MORBs) [*Hickey-Vargas*, 1989; *Ishizuka et al.*, 2006; *Meijer*, 1980; *Sun and McDonough*, 1989; *Taylor et al.*, 1994]. Compared with other plutonic suites from the northern IBM (Komahashi-Daini Seamount on the Kyushu-Palau Ridge) [*Haraguchi et al.*, 2003] and the Tanzawa Complex, Southern Honshu [*Kawate and Arima*, 1998], RD63 also has lower $TiO_2$, but a similar range of $SiO_2$ (~49–78 wt %) and other major oxides. These low $TiO_2$ contents link the dredge RD63 and RD64 rocks with boninites and boninite series rocks which have $SiO_2$ of 52–60% $SiO_2$ and notably low $TiO_2$ of 0.1–0.6% (Figure 2). The wide range of $SiO_2$ contents in the RD63 suite is similar to that observed in differentiated boninite lavas. For example, boninite-derived dacites from Chichijima reach 68% $SiO_2$ and rhyolites reach 78%. On major element diagrams, the differentiated boninite lavas and RD63 plutonic rocks overlap, both having notably low $TiO_2$

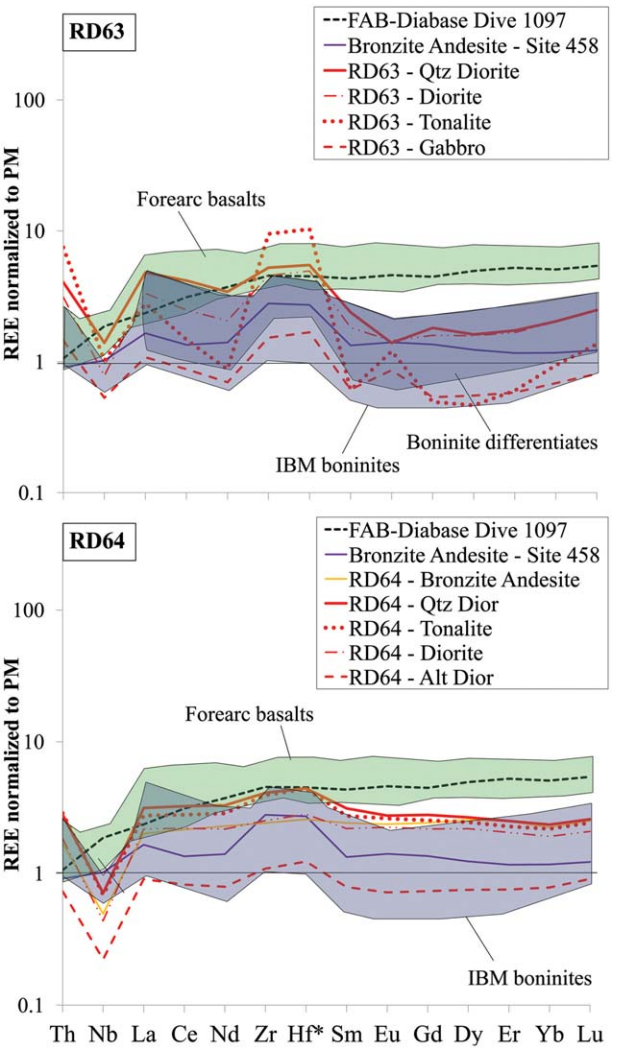


**Figure 3.** Primitive mantle normalized rare earth elements (REE) and other trace elements. In the RD63 diagram, the red lines represent gabbro, diorite, quartz diorite, and tonalite from RD63. The gabbro and tonalite have lowest REE abundances and positive Eu anomalies, whereas diorite and quartz diorite have higher REE abundances and either negative or no Eu anomaly. In the RD64 diagram, the red lines represent a gabbro, quartz diorite, diorite, and tonalite. The orange line represents a bronzite andesite from RD64 as a comparison to a bronzite andesite from Site 458 (458 24-1wr) [*Reagan et al.*, 2010], which is a purple line on both diagrams. Shaded fields in both diagrams are FABs (green), boninites (blue), differentiated boninites (darker blue in RD63). FABs are from DSDP Sites 458 and 459 and Mariana fore-arc submersible dive sites [*Reagan et al.*, 2010] and a representative FAB (1097-3) is shown by a dashed black line. Boninites are from Chichijima, Guam, DSDP Site 458, and ODP Site 786, and dredges and dives from the southern Mariana forearc [*Hickey-Vargas and Reagan*, 1987; *Pearce et al.*, 1999; *Reagan et al.*, 2010; *Taylor et al.*, 1994]. Boninite differentiates (andesites, dacites, rhyolites) are from Chichijima [*Taylor et al.*, 1994]. Elements with an asterisk (*) indicate that they were not reported or analyzed and therefore are an average of the adjacent elements. The boninite differentiates from Chichijima in *Taylor et al.* [1994] did not include Th or Nb values and were omitted in the darker blue field. REEs were normalized based on the primitive mantle value of *Sun and McDonough* [1989].

(Figure 2d), and differing only in that the plutonic suite has uniformly higher $Al_2O_3$ for a given $SiO_2$ (Figure 2e). At high $SiO_2$ (73–78% $SiO_2$), the RD63 also overlap in $TiO_2$ with the range for nonboninite related early IBM rhyolites from Saipan [*Meijer*, 1980; *Meijer et al.*, 1983; *Reagan et al.*, 2008] and Quaternary rhyolites from the northern IBM [*Tamura et al.*, 2009].

### 5.2. Trace Elements

Like most arc rocks, both suites exhibit a pronounced negative Nb anomaly (normalized La/Nb = 1.3–5.7 for RD63 and 3.7–5.3 for RD64), and are enriched in Th relative to Nb (Th/Nb = 2.6–10.1). The REE patterns of RD63 rocks (Figure 3) are enriched in both L(light)REE and H(heavy)REE (primitive mantle normalized La/Sm = 1.3–4.6 and Yb/Sm = 0.9–1.6), resulting in a "U"-shaped REE pattern resembling that of boninites from the IBM. The dredge RD63 plutonics exhibit both positive and negative Eu anomalies. Gabbros have a Eu/Eu* of 1.5–2.4, whereas diorites-quartz diorites have Eu/Eu* of 0.70–1.08, and the tonalites have a large positive anomaly (up to 2.2). All dredge RD63 rocks exhibit a conspicuous positive Hf-Zr anomaly relative to REE (Figure 3), which is a unique characteristic of boninites not found in other island arc rocks [e.g., *Pearce et al.*, 1999]. The Hf-Zr anomaly becomes increasingly positive relative to middle REE as $SiO_2$ content increases (Figures 3a and 6). Dredge RD64 rocks have flat REE patterns and some but not all exhibit slight positive Hf and Zr anomalies relative to REE (Figure 3b). Interestingly, neither FABs nor the bronzite andesites from Site 458 on the Mariana forearc exhibit pronounced negative Nb anomalies or Th enrichment (Figure 3), as do boninites and RD63 and RD64 rocks.

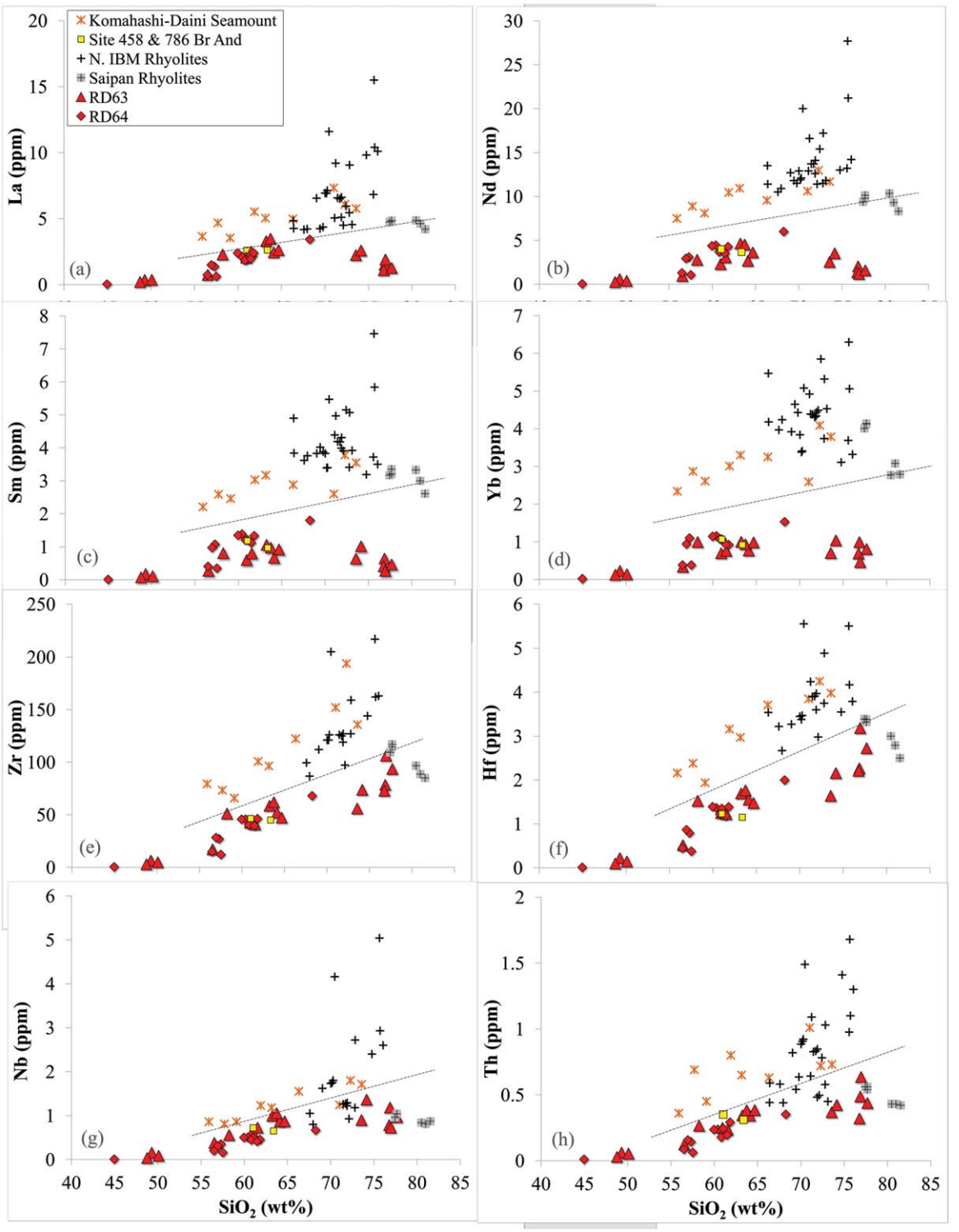


**Figure 4.** Trace elements (REEs and HFSEs) ppm versus $SiO_2$ (wt %). REE: La, Sm, Nd, and Yb and HFSE: Zr, Hf, Nb, and Th plotted versus $SiO_2$ to compare how the trace elements behave as differentiation occurs in intermediate and felsic rocks. Rocks from RD63 and RD64 (this study) are compared with Quaternary dacites and rhyolites from the northern IBM [*Tamura et al*., 2009], Saipan rhyolites [*Reagan et al*., 2008]; and plutonic rocks from the Komahashi-Daini Seamount tonalites [*Haraguchi et al*., 2003]. The dashed line through the data represents a rough boundary between the RD63 and RD64 and other intermediate and felsic rocks.

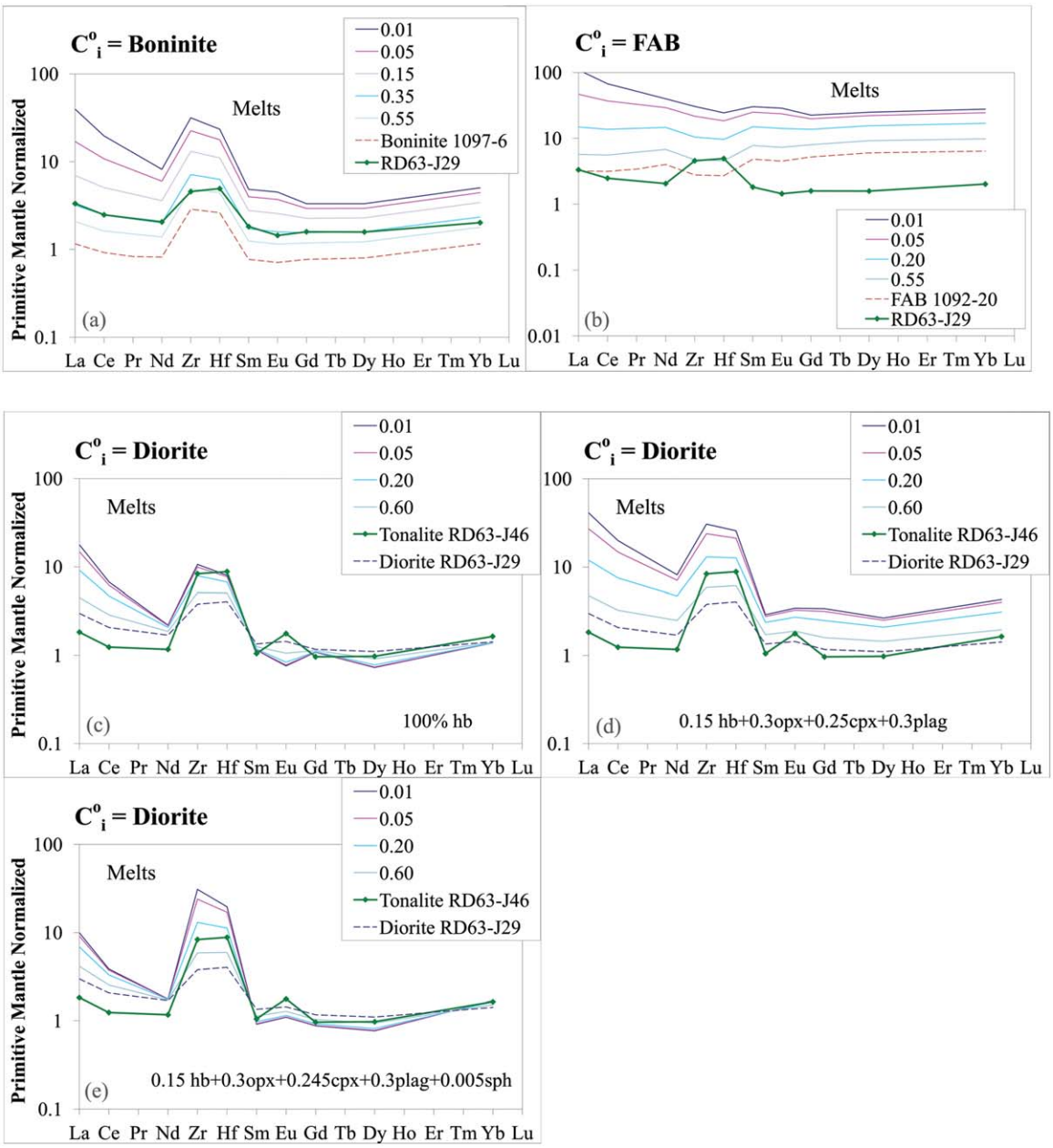


**Figure 5.** Quantitative trace element modeling of various sources (boninite and FAB: *Reagan et al.* [2010] and diorite: this study) showing the resultant REE, Zr, and Hf abundances compared with intermediate and felsic plutonic samples from RD63. The REE signature is inherited from boninite during melting and crystallization, a signature unlike FAB. The high Zr-Hf anomaly found in high silica tonalites can be achieved by either crystallization or partial melting, including amphibole and trace sphene. Partition coefficients used in the model are from the GERM website (EarthRef.org).

The behavior of REEs and Zr, Hf, Nb, and Th is displayed in more detail in several other trace element plots. Overall, RD63 and RD64 rocks have systematically lower concentrations of REE, Zr, Hf, Nb, and Th across their entire range of 55–78% $SiO_2$ compared with recent IBM silicic rocks and the plutonic suite from Komahashi-Daini Seamount, and this difference is most pronounced for middle (Nd, Sm) and heavy REE (Yb). In all suites, incompatible trace element abundances increase with $SiO_2$ up to about 70%. At that point, recent northern IBM silicic volcanic rocks and the Komahashi-Daini Seamount suite continue to increase for these eight elements, whereas abundances of REE in RD63 and RD64 decrease, mimicking the behavior of $TiO_2$ (Figure 2). The decoupling of REE from Zr and Hf is evident here in the RD63 and RD64 plutonic suites (Figure 6). Zr/Sm ratios in gabbros from RD63 and RD64, like those of boninites, are generally higher than

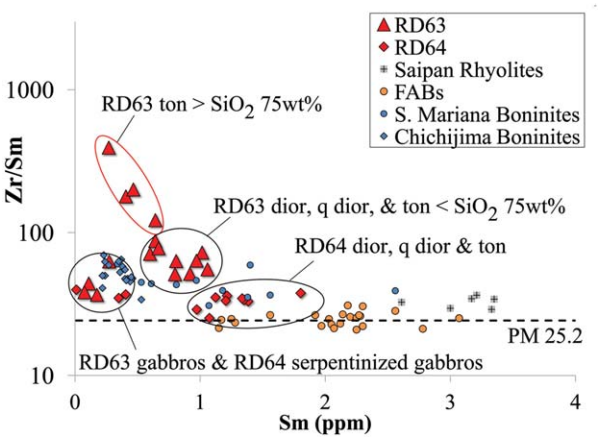


**Figure 6.** Variation of Zr/Sm ratios in RD63 and RD64 plutonic suites compared with other volcanic and plutonic suites from the early IBM, and the relationship of Zr/Sm to Sm abundances. FABs (fore-arc basalts) are from *Reagan et al.* [2010]; Saipan rhyolites are from *Reagan et al.* [2008]; and boninites are from Chichijima [*Taylor et al.*, 1994] and the southern Mariana forearc [*Reagan et al.*, 2010]. The black dashed line represents the Zr/Sm composition of primitive mantle reported by *Sun and McDonough* [1989]. Abbreviations of lithologies are as follows: ton = tonalite; q dior = quartz diorite; and dior = diorite.

those in FABs (average 25), normal arc basalts, MORBs, and primitive mantle. RD63 diorites, quartz diorites, and tonalites with $<75\%$ $SiO_2$ have even higher Zr/Sm (average 58), whereas the most silicic tonalites, those having a granophyric texture, range from 71 to 394. The diorites, quartz diorites, and tonalites in RD63 have higher Zr/Sm than any other rock (Figure 6) and the Zr/Sm increases significantly in tonalites with $SiO_2 > 75$ wt %. This pattern of high Zr/Sm in RD63 diorites, quartz diorites, and tonalites coincides with depleted trace element contents for all RD63 samples (even compared to RD64 samples), and notably a pronounced decrease in Sm (and other REE) contents in granophyric tonalites with $SiO_2 > 75$ wt % (Figure 4). Diorites, quartz diorites, and tonalites from RD64 do not show this trend, although Zr/Sm ratios are generally higher than primitive mantle.

### 5.3. Sr, Nd, Hf, and Pb Isotope Data

On a plot of initial $\varepsilon_{Nd}$ versus initial $^{87}Sr/^{86}Sr$ (Figure 7a), the RD63 and RD64 rocks lie within the field for IBM arc boninites at lower $\varepsilon_{Nd}$ and generally higher $^{87}Sr/^{86}Sr$ than FABs or the early IBM arc lavas. RD64 rocks have systematically higher $\varepsilon_{Nd}$ compared with RD63. Within each suite, there is no systematic change in Sr or Nd isotope ratios with bulk composition or normative lithology. On the plot of initial $\varepsilon_{Hf}$ versus $\varepsilon_{Nd}$ (Figure 7b), the RD63 and RD64 rocks also lie near the fields of IBM boninites, distinct from the higher $\varepsilon_{Nd}$ of FABs and the early IBM arc. $\varepsilon_{Hf}$ values are generally lower in boninites and the RD63 and RD64 samples compared with FABs and early IBM arc lavas. Notably, however, nearly all FABs and early IBM rocks fall in the field of Indian MORB [*Pearce et al.*, 1999]. On plots of initial Pb isotope ratios (Figures 7c and 7d), RD63 and RD64 rocks again lie with IBM arc boninites in a cluster from $^{206}Pb/^{204}Pb$ of 18.5–18.9, and they overlap with the more radiogenic end of FABs and the early IBM arc. RD64 samples have slightly lower $^{208}Pb/^{204}Pb$ compared with RD63 (Figure 7d), and systematically lower $^{207}Pb/^{204}Pb$, which fall below the NHRL. Some RD63 samples have Pb isotopic compositions that are like boninites from Chichijima in the northern IBM, which trend upward away from the NHRL, whereas others fall with boninites from ODP Site 786, Guam and the southern IBM which trend along the NHRL. Similar to Sr and Nd isotopes, there is no systematic change in Hf or Pb isotopes with bulk composition or normative lithology within each suite.

## 6. Discussion

### 6.1. Origin of Dredged Suites and Relationship to Volcanic Suites

The recovery of plutonic rocks from the Mariana forearc, first reported by *Bloomer* [1983] and *Bloomer and Hawkins* [1987], is a puzzling discovery because it implies that deep layers of the arc crust are exposed on the inner Mariana Trench slope. This requires extensive erosive or extensional forces to expose rocks which otherwise are several kilometers beneath the surface (based on P-wave velocities). The hypothesis that lavas from the IBM forearc likely represent the first volcanic products of subduction initiation, has led to many studies addressing the origin and age of those lavas through petrologic, geochemical, and geochronological analyses [*Bloomer*, 1983; *Fryer et al.*, 1990; *Hawkins et al.*, 1984; *Hickey-Vargas and Reagan*, 1987; *Ishizuka et al.*, 1998, 2006; *Kaneoka et al.*, 1970; *Meijer et al.*, 1983; *Mitchell et al.*, 1992; *Natland and Tarney*, 1981; *Pearce et al.*, 1999, 1992; *Reagan and Meijer*, 1984; *Stern and Bloomer*, 1992; *Taylor and Mitchell*, 1992]. Recent efforts to

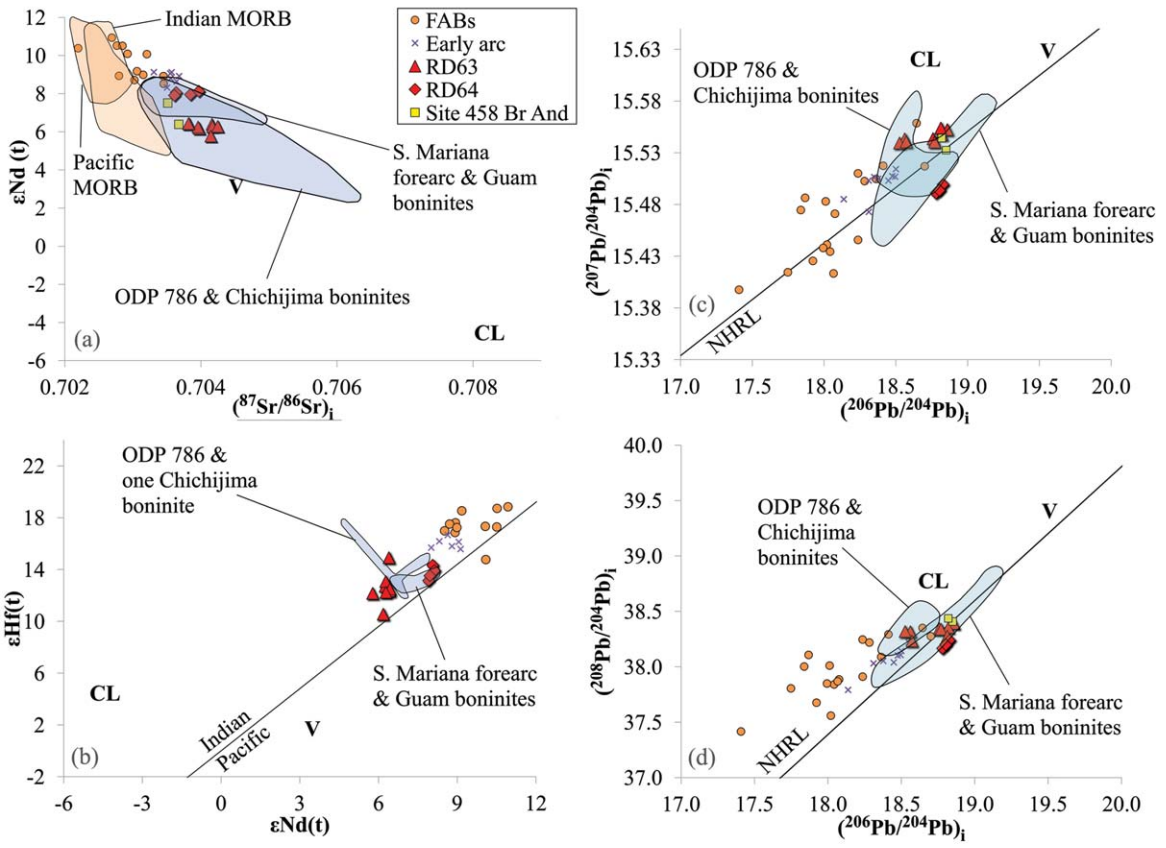


**Figure 7.** Initial isotopic compositions of rocks from RD63 and RD64 compared with other igneous rocks from the southern Mariana arc. An age of 50 Ma was assumed for the RD63 and RD64 dredge samples, similar to that of the dated boninite volcanics. The other rocks on the plots were corrected using their ages inferred from radiometric dating. Data sources for these plots are the same as previous figures. The MORB field in (a) was compiled from the literature. Sediment compositions for the Pacific plate in the vicinity of the IBM arc are represented by average volcaniclastic sediments (V) and clay (CL) from *Pearce et al.* [1999] and *Elliott et al.* [1997]. NHRL in (b) and (d) is the Northern Hemisphere Reference Line from *Hart* [1984], and the Indian-Pacific "boundary" in (c) is from *Pearce et al.* [1999].

fully sample the trench slope, and the synthesis of the volcanic stratigraphy, petrology, and geochemistry [*Reagan et al.*, 2008, 2010], provide a solid context for interpreting the origin of these nearby, rare plutonic rocks. Our geochemical data indicate that the plutonic rocks from dredges RD63 and RD64 are related to the infant arc volcanic sequence. The geochemical data, primarily the isotopic ratios, suggest that these dredges are distinct from each other even though they are from similar depths in the forearc. In addition, the uniform Sr, Nd, Pb, and Hf isotopic composition of samples within each dredge suggests that the samples are genetically related to one another and can be interpreted in terms of crystallization and melting processes.

Major and trace element evidence clearly shows that the RD63 plutonic suite is related to boninite and boninite-like rocks from the IBM forearc, including their characteristic low $TiO_2$ content, U-shaped REE patterns and excess Zr and Hf compared with middle REEs. The Sr, Nd, Hf, and Pb isotopic data are consistent with a boninite parent. Isotope ratios for the RD63 and RD64 plutonic suites have distinctly lower $^{143}Nd/^{144}Nd$ and higher $^{206}Pb/^{204}Pb$ than most FABs, low-K tholeiitic, and calc-alkaline volcanic rocks from the early IBM arc, and all plot within fields for IBM arc boninites. Interestingly, plutonic rocks from RD63 have isotope ratios most similar to "bronzite andesite" boninite derivatives from DSDP Site 458 and boninites from Chichijima in the Izu-Bonin segment, rather than to boninite-like rocks sampled from Guam and the nearby upper trench. Compared to the latter boninites, $^{143}Nd/^{144}Nd$ and $^{206}Pb/^{204}Pb$ ratios are lower. These differences may reflect a difference in the sediment component in the boninite parent for the RD63 suite. Differences in $^{206}Pb/^{204}Pb$ ratios in IBM arc volcanics have been widely attributed to sourcing of Pb from seamount-derived volcaniclastic sediment (V in Figure 7) versus a source from dominantly pelagic sediment (CL in Figure 7) [*Elliott et al.*, 1997]. Our interpretation is that the boninite parent magma of the RD63 suite incorporated more Pb and Nd from pelagic sediment, resulting in lower $^{143}Nd/^{144}Nd$, lower $^{206}Pb/^{204}Pb$ and higher $^{207}Pb/^{204}Pb$ and $^{208}Pb/^{204}Pb$ than boninites from the upper trench wall and Guam,

and more similar to boninites from Chichijima. FABs have much less radiogenic Pb and Sr isotope ratios than boninites and related plutonics everywhere within the early IBM, a feature which was interpreted by *Reagan et al*. [2010] to indicate there is little to no subduction influence in FABs compared with boninites. Boninites and the related RD63 and RD64 plutonics also have unradiogenic Nd and Hf isotope ratios compared to FABs which may have been acquired from a distinct mantle source that was not incorporated into the FAB melts between 48 and 52 Ma [*Reagan et al*., 2010]. Alternatively, the depleted boninite source may have been affected by a small contribution from pelagic sediment at the early stages of subduction, resulting in lower $^{143}Nd/^{144}Nd$ (Figure 7).

Plutonic rocks from RD64 have $^{143}Nd/^{144}Nd$ in the uppermost range for IBM boninites, and overlap in $^{87}Sr/^{86}Sr$, $^{176}Hf/^{177}Hf$, and $^{206}Pb/^{204}Pb$ with those from Guam and the nearby upper trench. $^{207}Pb/^{204}Pb$ and $^{208}Pb/^{204}Pb$ are slightly lower compared with those fields, and may reflect a slightly different composition for the seamount-derived volcaniclastic sediment end-member (Figure 7) with lower $^{207}Pb/^{204}Pb$ and $^{208}Pb/^{204}Pb$ compared with those currently found on the Pacific plate.

### 6.2. Boninite Differentiation to Form the Plutonic Suites

Potential differentiation pathways for boninite magma can be inferred from differentiated boninite volcanic suites [*Hickey-Vargas*, 1989; *Ishizuka et al*., 2006; *Kuroda et al*., 1988; *Kushiro*, 1981; *Natland and Tarney*, 1981; *Taylor and Nesbitt*, 1995; *Taylor et al*., 2003, 1994; *Umino*, 1985] and observed boninite mineralogy. Major element trends (Figure 2) for boninite liquids are initially driven by crystallization of orthopyroxene, as shown by decreasing MgO and $FeO_T$, and increasing $Al_2O_3$, CaO, and $TiO_2$ at relatively constant $SiO_2$ of 58%. At this $SiO_2$ content, trends approach the field for RD63 plutonic rocks at 16% $Al_2O_3$, 8% FeO, 5% MgO, and 8% CaO. These major element abundances are similar to those of boninite-derived bronzite andesites found at DSDP Site 458 and on Chichijima, which contain orthopyroxene and rare clinopyroxene phenocrysts, and plagioclase microlites. Our proposed crystallization scenario for the RD63 plutonic suite is: (1) crystallization of opx $\pm$ cpx from boninite magma, until plagioclase saturation is reached, followed by (2) accumulation of plagioclase and pyroxene to form rocks $<$58% $SiO_2$ (Figure 2) and (3) plagioclase $\pm$ pyroxene crystallization for most of the trend $>$58% $SiO_2$ (Figure 2).

The abundance of plagioclase in the RD63 plutonic suite contrasts with the typical characteristics of boninite volcanics, where plagioclase is rarely an abundant mineral except at extreme $SiO_2$ enrichment (i.e., perlitic dacite and rhyolite from Chichijima) [*Kuroda et al*., 1988]. Possibly, in the case of the RD63 plutonic rocks, the ascent of boninitic magma was stalled in the midcrust to upper crust, allowing magma degassing and extended low-pressure crystallization, both of which favor plagioclase stability. Since there are no plutonic rocks coincident with the orthopyroxene crystallization part of the boninite trend, it is probable that a MgO-poor, $Al_2O_3$-rich "bronzite andesite" precursor separated from the ascending boninite magmas and then underwent accumulation to form gabbro and differentiation to the extreme compositions represented by the tonalites. Gabbro cumulates have higher $Al_2O_3$ and positive Eu anomalies due to high modal amounts of plagioclase feldspar (Figure 3). Granophyric textures in four RD63 tonalite samples are indicative of quartz and feldspar crystallizing simultaneously, such as when a silicate melt is at the eutectic point or when a silicic liquid is undercooled [*Fenn*, 1986; *Lentz and Fowler*, 1992; *London et al*., 1989; *Lowenstern et al*., 1997]. This is often the case in plutons at shallow depths during late stage crystallization, or in the first phase of melting of a mafic rock, which in this case could be the previously emplaced boninite crust. Since we have no constraints on the size or original location of the suite, the plutonic rocks may have been small, heterogeneous pods or masses in the arc crust, or alternatively, kilometer-sized intrusions with gabbroic through tonalitic lithologies.

Rare earth element (REE) patterns of rocks from the plutonic suites from the southern Mariana Trench have the U-shaped pattern that is characteristic of boninites from the IBM arc, which has been attributed to partial melting of depleted mantle peridotite enriched in LREE by metasomatic fluids [*Hickey-Vargas and Reagan*, 1987; *Hickey and Frey*, 1982; *Pearce et al*., 1992; *Reagan and Meijer*, 1984]. Bronzite andesites from DSDP Site 458 and Chichijima, differentiates that are boninite like, and all types of plutonics from RD63 and RD64, with the exception of some gabbros, also have U-shaped patterns and they fall within these fields. The Eu/Eu* (i.e., the positive Eu anomaly) in the gabbroic cumulates supports plagioclase accumulation from a melt composition approximately similar to the DSDP Site 458 bronzite andesites. The unique REE patterns and elevated Zr/Sm and Hf/Sm of boninites are also found in diorites of the RD63 suite, confirming their origin

from a boninite differentiate as described above. At this point in the crystallization sequence, none of the likely fractionating minerals, orthopyroxene, clinopyroxene, or plagioclase, can produce U-shaped REE patterns or elevated Zr/Sm if not inherited from the parental magma.

The increased decoupling of the high field strength elements (HFSEs) from REEs with differentiation, particularly in high silica tonalites, appears to result from extraction of the REE rather than enrichment of Zr and Hf (Figures 4 and 6). Detailed major and trace element modeling calculations for crystallization and partial melting of three possible magma or rock precursors: (1) boninite, (2) FAB, and (3) diorite confirm that a differentiated boninite magma or boninite rock source is essential for the plutonic suite (Figure 5). Crystallization of intermediate boninite magma is the most likely first step, and this produces gabbro, diorite, and quartz diorite. In a second step leading to tonalite, both crystallization and partial melting are possible. For both crystallization and partial melting, hornblende and in some cases an accessory mineral such as apatite or sphene is required to account for the diminishing REE content and increasing Zr/Sm. The accessory mineral sphene was included in the trace element models (Figure 5) and it has been shown to have a somewhat large stability field at low to moderate P-T [*Hunt and Kerrick*, 1977]. Significantly, in all scenarios, a boninite precursor, magma or rock, is the only starting composition that results in HFSE/REE patterns similar to RD63 and RD64 plutonics (Figure 5), confirming that the plutonics have inherited this signature from boninites in this location.

### 6.3. Comparison With Other IBM-Related Plutonic Suites and the "Midcrustal" Felsic Layer

With the exception of $TiO_2$, the intermediate to felsic plutonic rocks of RD63 and RD64 (>60% $SiO_2$) plot within the major oxide differentiation trends of other rare IBM-related plutonic suites, i.e., rocks dredged from Komahashi-Daini Seamount on the Kyushu-Palau Ridge and tonalites and gabbros found in the Tanzawa Plutonic Complex (TPC) in Honshu, Japan. CaO contents in the inner trench slope suites are slightly more scattered and some MgO contents are higher at the low $SiO_2$ end. The tonalites from the Komahashi-Daini Seamount were dated at 38–37 Ma (K-Ar) and hypothesized to have formed by fractional crystallization from a low-K basaltic melt prior to the rifting of the early IBM arc [*Haraguchi et al*., 2003, 2012; *Shibata et al*., 1977]. The TPC plutonics have recently been dated using U-Pb in zircon at 9–4 Ma, which indicates that the plutons are a result of syncollisional magmatism of the Honshu-TPC block with the northern IBM arc [*Tani et al*., 2012]. The complex is explained by partial melting of a hydrous calc-alkaline basaltic lower crust [*Kawate and Arima*, 1998; *Tani et al*., 2012]. Despite the differences in tectonomagmatic setting among these locations: (1) normal subduction zone magmatism (Kyushu-Palau Ridge), (2) collision and lower crustal melting (Tanzawa), and (3) arc initiation (RD63 and RD64), the intermediate to felsic plutonic rocks have broadly similar major element and mineralogical characteristics and would be difficult to distinguish on this basis. Any or all of these types of plutonic suites could be incorporated into the midcrustal low seismic velocity layer identified by *Suyehiro et al*. [1996] and *Takahashi et al*. [2008], although it is most likely that boninite derivatives form only a small proportion based on the abundance of boninite lavas.

On the other hand, there are many petrologic similarities between the RD63 plutonic rocks and plutonic rocks found in some suprasubduction zone (SSZ) ophiolites, including rocks referred to as plagiogranites by *Dilek and Thy* [2006] and *Rollinson* [2009]. Several recent studies [*Dilek and Thy*, 2009; *Dilek and Furnes*, 2009; *Stern et al*., 2012; *Whattam and Stern*, 2011] have linked the occurrence of boninite in arc initiation suites to the concept that boninite-bearing SSZ ophiolites are preserved sections of forearc. Assuming our identification of the RD63 and RD64 plutonic suites as boninite derivatives is correct, the occurrence of plagiogranites with comparable major and trace element features in a SSZ ophiolite could confirm its formation in a forearc environment during the initiation of subduction even if boninites are not found.

### 6.4. Geologic and Petrogenetic Synthesis

Based on an overview of early IBM arc history, a possible origin of the RD63 and RD64 dredge samples can be described as follows. At 48–52 Ma, after subduction had recently initiated along the southern Mariana trench, boninite magmas were generated and erupted in an extensional environment [*Bloomer and Hawkins*, 1987; *Bloomer et al*., 1995; *Meijer*, 1980; *Reagan and Meijer*, 1984; *Stern*, 2004; *Stern and Bloomer*, 1992]. Boninite magma was generated at relatively shallow levels in the lithosphere by decompression of depleted mantle and with a large flux of hydrous fluid from the downgoing Pacific plate [*Ishizuka et al*., 2006; *Pearce et al*., 1999, 1992]. FABs, the earliest lavas to erupt following plate subsidence, have varying geochemical characteristics, but are unlike boninites or the RD63 or RD64 plutonic suites. *Reagan et al*. [2010]

hypothesized two scenarios for the development of the depleted mantle source responsible for early IBM magmas: (1) mantle was depleted during formation of the West Philippine Basin, which was later remelted as the Pacific plate began to subside and (2) mantle beneath the continent of Asia became detached and through large-scale mantle convection came to rest near the infant Mariana trench. The former explanation for the depleted source is not ideal because the radiogenic Nd isotopic composition of FABs does not match those of West Philippine Basin basalts, nor does it explicitly account for differences in Nd and Hf isotope ratios between FABs and boninites. The latter explanation attributes the source of the Indian Ocean MORB signature in the Philippine Sea plate to mobilized sub-Asian mantle which provides the Nd, Hf, and Pb isotope domains observed for the entire IBM arc-back-arc system, in addition to potentially providing the force to initiate convergence between the Philippine Sea and Pacific plates.

Most boninite magma was erupted at volcanic centers whose remnants are located in the present-day forearc. Storage and differentiation of the boninite magma in at least two locations produced the plutonic suites described in this study. Crystallization of intermediate boninite magma formed gabbro cumulates, consisting primarily of plagioclase, orthopyroxene, and magnetite, whilst boninite lavas were erupted at the surface. Continued differentiation of the magma by separation of these minerals and hornblende produced progressively more felsic intrusive rocks (diorite, quartz diorite, tonalite), which may or may not have had volcanic equivalents. It is also possible that the most felsic rocks formed by partial melting of more mafic boninite rock, leaving a residue containing hornblende and a REE-rich accessory mineral. In this latter case, melting can only have occurred in the forearc during the interval when FABs or boninites were being generated (50–43 Ma), since there is no subsequent source of heat to cause partial melting of the fore-arc crust. Therefore, even without supporting geochronological data, it is likely that the boninite-like plutonic suites in the southern Mariana forearc formed from shallowly emplaced and differentiating boninite magma bodies, with the most felsic members formed by extreme differentiation and/or by partial melting of boninite crust, around the time of subduction initiation.

Exposure of the plutonic rocks on the trench slope near Guam may have been facilitated by tectonic erosion of the overriding plate, as the Mariana forearc here is as much as 50 km narrower than at higher latitudes. Thus more of the arc lithospheric crust would be exposed than in other parts of the arc. Normal faults are also an effective mechanism for midcrustal exposure. RD64 was recovered from a fault scarp, and the serpentine mud volcano located at RD63 may have developed over a fault acting as a conduit for fluids.

## 7. Conclusions

(1) Plutonic and hypabyssal rocks were recovered in two deep dredges (7800–8100 m) in the southern Mariana forearc (University of Hawai'i R/V Kana Keoki 81-06-26, RD63 and RD64). (2) RD63 and RD64 include felsic, intermediate, and mafic rocks that are boninite derivatives based on major and trace element and isotopic considerations. RD64 also includes volcanic and hypabyssal rocks that are chemically intermediate between boninite and arc tholeiite lava. (3) The RD63 suite is distinct from other highly differentiated rocks suites from the IBM system, such as tonalites dredged from the Komahashi-Daini Seamount, Kyushu-Palau Ridge, and volcanic centers producing rhyolites in the northern IBM and Saipan. The characteristic U-shaped REE patterns and elevated Zr/Sm and Hf/Sm of the intermediate plutonic rocks are inherited from the boninite parental magmas, but these are modified by further crystallization and/or late stage partial melting to form tonalite. (4) The association of the plutonic rock suite with boninite indicates that the formation of intermediate and felsic arc crust may begin at the earliest stages of intraoceanic island arc development. (5) The exposure of these plutonic rocks, which may be part of a seismically imaged low-velocity midcrustal layer, was facilitated by tectonic erosion and normal faulting of the fore-arc lithosphere.

**Acknowledgments**

This research was carried out with funds granted to us by NSF grant OCE 09028144. Afi Sachi-Kocher (NHMFL) and Adriana Potra (FIU) are thanked for their help and guidance with the sample dissolution procedures and isotope separation and analysis at NHMFL.

## References

Bénard, A., and D. A. Ionov (2012), A new petrogenetic model for low-Ca boninites: Evidence from veined sub-arc xenoliths on melt-mantle interaction and melt fractionation, *Geochem. Geophys. Geosyst.*, *13*, Q0AF05, doi:10.1029/2012GC004145.

Blichert-Toft, J., and F. Albarède (1997), The Lu-Hf isotope geochemistry of chondrites and the evolution of the mantle-crust system, *Earth Planet. Sci. Lett.*, *148*, 242–258.

Bloomer, S. H. (1983), Distribution and origin of igneous rocks from the landward slopes of the Mariana Trench: Implications for its structure and evolution, *J. Geophys. Res.*, *88*, 7411–7428.

Bloomer, S. H., and J. H. Hawkins (1987), Petrology and geochemistry of boninite series volcanic rocks from the Mariana Trench, *Contrib. Mineral. Petrol.*, *97*, 361–377.

Bloomer, S. H., B. Taylor, C. J. MacLeod, R. J. Stern, P. Fryer, J. H. Hawkins, and L. Johnson (1995), Early arc volcanism and the ophiolite problem: A prospective from drilling in the western Pacific, in *Active Margins and Marginal Basins of the Western Pacific, Geophys. Monogr. Ser.*, vol. *88*, edited by B. Taylor and J. Natland, pp. 1–30, AGU, Washington, D. C.

Clague, D. A., and G. B. Dalrymple (1987), The Hawaiian-Emperor Seamount Chain, Part I, geologic evolution, *U.S. Geol. Surv. Prof. Pap.*, *1350*, 5–54.

Cosca, M. A., R. J. Arculus, J. A. Pearce, and J. G. Mitchell (1998), $^{40}Ar/^{39}Ar$ and K-Ar geochronological age constraints for the inception and early evolution of the Izu-Bonin-Mariana arc system, *Isl. Arc*, *7*, 579–595.

Dilek, Y., and H. Furnes (2009), Structure and geochemistry of Tethyan ophiolites and their petrogenesis in subduction rollback systems, *Lithos*, *113*, 1–20.

Dilek, Y., and P. Thy (2006), Age and petrogenesis of plagiogranite intrusions in the Ankara melange, central Turkey, *Isl. Arc*, *15*, 44–57.

Dilek, Y., and P. Thy (2009), Island arc tholeiite to boninitic melt evolution of the Cretaceous Kizildag (Turkey) ophiolite: Model for multi-stage early arc-forearc magmatism in Tethyan subduction factories, *Lithos*, *113*, 68–87.

Elliott, T., T. Plank, A. Zindler, W. White, and B. Bourdon (1997), Element transport from slab to volcanic front at the Mariana arc, *J. Geophys. Res.*, *102*, 14,991–15,019.

Fenn, P. M. (1986), On the origin of graphic granite, *Am. Mineral.*, *71*, 325–330.

Fryer, P., et al. (1990), Proceedings ODP science results covering Leg 125 of the cruises of the drilling vessel JOIDES resolution, in *Proceedings of the Ocean Drilling Program, Scientific Results*, vol. *125*, edited by S. K. Stewart, Ocean Drill. Program, College Station, Tex.

Gill, J. B. (1981), *Orogenic Andesites and Plate Tectonics*, Springer, Berlin.

Gill, J. B., R. N. Hiscott, and P. Vidal (1994), Turbidite geochemistry and evolution of the Izu-Bonin arc and continents, *Lithos*, *33*, 135–168.

Hacker, B. R., G. A. Abers, and S. M. Peacock (2003), Subduction factory: 1. Theoretical mineralogy, densities, seismic wave speeds, and $H_2O$ contents, *J. Geophys. Res.*, *108*(B1), 2029, doi:10.1029/2001JB001127.

Haraguchi, S., T. Ishii, J.-I. Kimura, and Y. Ohara (2003), Formation of tonalite from basaltic magma at the Komahashi-Daini Seamount, northern Kyuhu-Palau Ridge in the Philippine Sea, and growth of Izu-Ogasawara (Bonin)-Mariana arc crust, *Contrib. Mineral. Petrol.*, *145*, 151–168.

Haraguchi, S., T. Ishii, J.-I. Kimura, and Y. Kato (2012), The early Miocene (~25 Ma) volcanism in the northern Kyushu-Palau Ridge, enriched mantle source injection during rifting prior to the Shikoku backarc basin opening, *Contrib. Mineral. Petrol.*, *163*, 483–504.

Hart, S. R. (1984), A large-scale isotope anomaly in the Southern Hemisphere mantle, *Nature*, *309*, 753–757.

Hart, S. R., and C. Brooks (1977), The geochemistry and evolution of the early Precambrian mantle, *Contrib. Mineral. Petrol.*, *61*, 109–128.

Hawkins, J. W., S. H. Bloomer, C. A. Evans, and J. T. Melchior (1984), Evolution of intra-oceanic arc-trench systems, *Tectonophysics*, *102*, 175–205.

Hickey, R., and F. A. Frey (1982), Geochemical characteristics of boninite series volcanics: Implications for their source, *Geochim. Cosmochim. Acta*, *46*, 2099–2116.

Hickey-Vargas, R. (1989), Boninites and tholeiites from DSDP Site 458, Mariana Forearc, in *Boninites and Related Rocks*, edited by A. J. Crawford, pp. 339–356, Unwin Hyman, London, U. K.

Hickey-Vargas, R., and M. K. Reagan (1987), Temporal variation of isotope and rare earth element abundances in volcanic rocks from Guam: Implications for the evolution of the Mariana Arc, *Contrib. Mineral. Petrol.*, *97*, 497–508.

Hunt, J. A., and D. M. Kerrick (1977), The stability of sphene; experimental redetermination and geologic implications, *Geochim. Cosmochim. Acta*, *41*(2), 279–280.

Ishizuka, O., K. Uto, M. Yuasa, and A. G. Hochstaedter (1998), Preliminary K-Ar ages from seamount chains in the back-arc regoin of the Izu-Ogasawara arc, *Isl. Arc*, *7*, 408–421.

Ishizuka, O., et al. (2006), Early stages in the evolution of Izu-Bonin arc volcanism: New age, chemical and isotopic constraints, *Earth Planet. Sci. Lett.*, *250*(1–2), 385–401.

Ishizuka, O., K. Tani, M. Reagan, K. Kanayama, S. Umino, Y. Harigane, I. Sakamoto, Y. Miyajima, M. Yuasa, and D. J. Dunkley (2011), The timescales of subduction initiation and subsequent evolution of an oceanic island arc, *Earth Planet. Sci. Lett.*, *306*, 229–240.

Johnson, D. M., P. R. Hooper, and R. M. Conrey (1999), XRF analysis of rocks and minerals for major and trace elements on a single low dilution Li-tetraborate fused bead, *Adv. X-ray Anal.*, *41*, 843–867.

Kaneoka, I., N. Isshiki, and S. Zashu (1970), K-Ar ages of the Izu-Bonin Islands, *Geochem. J.*, *4*(2), 53–60.

Kawate, S., and M. Arima (1998), Petrogenesis of the Tanzawa plutonic complex, central Japan: Exposed felsic middle crust of the Izu-Bonin-Mariana arc, *Isl. Arc*, *7*, 342–358.

Kuroda, N., K. Shiraki, and H. Urano (1988), Ferropigeonite quartz dacites from Chichijima, Bonin islands: Latest differentiates from boninite-forming magma, *Contrib. Mineral. Petrol.*, *100*(2), 129–138.

Kushiro, I. (1981), Petrology of high-MgO bronzite andesite resembling boninite from Site 458 near the Mariana Trench, in *Initial Reports of the Deep Sea Drilling Project Leg 60*, edited by M. Lee and R. Powell, pp. 731–733, U.S. Gov. Print. Off., Washington, D. C.

Lentz, D. R., and A. D. Fowler (1992), A dynamic model for graphic quartz-feldspar intergrowths in granitic pegmatites in the southwestern Grenville Province, *Can. Mineral.*, *30*, 571–585.

London, D., G. B. I. Morgan, and R. L. Hervig (1989), Vapor-undersaturated experiments with Macusani glass + $H_2O$ at 200 MPa, and the internal differentiation of pegmatites, *Contrib. Mineral. Petrol.*, *102*, 1–17.

Lowenstern, J. B., M. A. Clynne, and T. D. Bullen (1997), Comagmatic A-type granophyre and rhyolite from the Alid volcanic center, Eritrea, northeast Africa, *J. Petrol.*, *38*(12), 1707–1721.

Mahoney, J. (1987), An isotopic survey of Pacific oceanic plateaus: Implications for their nature and origin, in *Seamounts, Islands, and Atolls, Geophys. Monogr. Ser.*, vol. *43*, edited by B. H. Keating et al., pp. 207–220, AGU, Washington, D. C.

Manhès, G., J.-P. Minster, and C. J. Allègre (1978), Comparative uranium-thorium-lead and rubidium-strontium of St. Severin amphoterite: Consequences for early solar system chronology, *Earth Planet. Sci. Lett.*, *39*, 14–24.

Meijer, A. (1980), Primitive arc volcanism and a boninite series: Examples from western Pacific island arcs, in *The Tectonic and Geologic Evolution of Southeast Asian Seas and Islands (Part II), Geophys. Monogr. Ser.*, vol. *23*, edited by D. E. Hayes, pp. 271–282, AGU, Washington, D. C.

Meijer, A., M. K. Reagan, H. Ellis, M. Shafiqullah, J. Sutter, P. Damon, and J. Kling (1983), Chronology of volcanic events in the eastern Philippine Sea, in *The Tectonic and Geologic Evolution of Southeast Asian Seas and Islands (Part II), Geophys. Monogr. Ser.*, vol. *27*, edited by D. E. Hayes, pp. 349–359, AGU, Washington, D. C.

Mitchell, J. G., D. W. Peate, B. J. Murton, J. A. Pearce, R. J. Arculus, and S. R. van der Laan (1992), K-Ar dating of samples from sites 782 and 786 (Leg 125); the Izu-Bonin forearc region, in *Proceedings of the Ocean Drilling Program Scientific Results*, vol. *125*, edited by S. K. Stewart, pp. 203–210, Ocean Drill. Program, College Station, Tex.

Münker, C., S. Weyer, E. Scherer, and K. Mezger (2001), Separation of high field strength elements (Nb, Ta, Zr, Hf) and Lu from rock samples for MC-ICPMS measurements, *Geochem. Geophys. Geosyst.*, *2*(12), 1064, doi:10.1029/2001GC000183.

Natland, J. H., and J. Tarney (1981), Petrologic evolution of the Mariana arc and back-arc basin system—A synthesis of drilling results in the south Philippine Sea, in *Initial Reports of the Deep Sea Drilling Project Leg 60*, edited by M. Lee and R. Powell, pp. 877–908, U.S. Gov. Print. Off., Washington, D. C.

Ohara, Y., et al. (2008), R/V Yokosuka YK08-08 Leg 2 Cruise: Structure and origin of the Mariana forearc and implications for the origin of continental crust: A Shinkai 6500 study of the southern Mariana forearc, cruise report, edited, Inst. for Res. on Earth Evol./Jpn. Agency for Mar. Earth Sci. and Technol., Japan.

Pearce, J. A., S. R. van der Laan, R. J. Arculus, B. J. Murton, and T. Ishii (1992), Boninite and harzburgite from ODP Leg 125 (Bonin-Mariana forearc): A case study in magma genesis during the initial stages of subduction, in *Proceedings of the Ocean Drilling Program, Scientific Results Leg 126*, edited by S. K. Stewart, pp. 623–659, Ocean Drill. Program, College Station, Tex.

Pearce, J. A., P. D. Kempton, G. M. Nowell, and S. R. Noble (1999), Hf-Nd element and isotope perspective on the nature and provenance of mantle and subduction components in western Pacific arc-basin systems, *J. Petrol.*, *40*(11), 1579–1611.

Reagan, M. K., and A. Meijer (1984), Geology and geochemistry of early arc-volcanic rocks from Guam, *Geol. Soc. Am. Bull.*, *95*, 701–713.

Reagan, M. K., B. Hanan, M. Heizler, B. Hartman, and R. Hickey-Vargas (2008), Petrogenesis of volcanic rocks from Saipan and Rota, Mariana Islands, and implications for the evolution of nascent island arcs, *J. Petrol.*, *49*(3), 441–464.

Reagan, M. K., et al. (2010), Fore-arc basalts and subduction initiation in the Izu-Bonin-Mariana system, *Geochem. Geophys. Geosyst.*, *11*, Q03X12, doi:10.1029/2009GC002871.

Reagan, M. K., W. C. McClelland, G. Girard, K. R. Goff, D. W. Peate, Y. Ohara, and R. J. Stern (2013), The geology of the southern Mariana fore-arc crust: Implications for the scale of Eocene volcanism in the western Pacific, *Earth Planet. Sci. Lett.*, *380*, 41–51.

Richard, P. N., N. Shimizu, and C. J. Allègre (1976), $^{143}Nd/^{144}Nd$, a natural tracer: An application to oceanic basalts, *Earth Planet. Sci. Lett.*, *31*, 269–278.

Rollinson, H. (2009), New models for the genesis of plagiogranites in the Oman ophiolite, *Lithos*, *112*, 603–614.

Salters, V. J. M. (1994), $^{176}Hf/^{177}Hf$ determination in small samples by a high temperature SIMS technique, *Anal. Chem.*, *66*, 4186–4189.

Salters, V. J. M., S. Mallick, S. R. Hart, C. E. Langmuir, and A. Stracke (2011), Domains of depleted mantle; new evidence from hafnium and neodymium isotopes, *Geochem. Geophys. Geosyst.*, *12*, Q08001, doi:10.1029/2011GC003617.

Sharp, W. D., and D. A. Clague (2006), 50-Ma initiation of Hawaiian-Emperor Bend records major change in Pacific plate motion, *Science*, *313*, 1281–1284.

Shibata, K., A. Mizuno, M. Yuasa, S. Uchida, and T. Nakagawa (1977), Further K-Ar dating of tonalite dredged from the Komahashi-Daini Seamount, *Bull. Geol. Surv. Jpn.*, *28*, 1–4.

Stern, R. J. (2004), Suubduction initiation: Spontaneous and induced, *Earth Planet. Sci. Lett.*, *226*, 275–292.

Stern, R. J., and S. H. Bloomer (1992), Subduction zone infancy: Examples from the Eocene Izu-Bonin-Mariana and Jurassic California arcs, *Geol. Soc. Am. Bull.*, *104*, 1621–1636.

Stern, R. J., M. Reagan, O. Ishizuka, Y. Ohara, and S. Whattam (2012), To understand subduction initiation, study forearc crust; to understand forearc crust, study ophiolites, *Lithosphere*, *4*, 469–483.

Sun, S.-S., and W. F. McDonough (1989), Chemical and isotopic systematics of oceanic basalts: Implications for mantle composition and processes, *Geol. Soc. Spec. Publ.*, *42*, 313–345.

Suyehiro, K., N. Takahashi, Y. Ariie, Y. Yokoi, R. Hino, M. Shinohara, T. Kanazawa, N. Hirata, H. Tokuyama, and A. Taira (1996), Continental crust, crustal underplating and low-Q upper mantle beneath an oceanic island arc, *Science*, *272*, 390–392.

Takahashi, N., K. Suyehiro, and M. Shinohara (1998), Implications from the seismic crustal structure of the northern Izu-Bonin arc, *Isl. Arc*, *7*, 383–394.

Takahashi, N., S. Kodaira, Y. Tatsumi, Y. Kaneda, and K. Suyehiro (2008), Structure and growth of the Izu-Bonin-Mariana arc crust: 1. Seismic constraint on crust and mantle structure of the Mariana arc-back-arc system, *J. Geophys. Res.*, *113*, B01104, doi:10.1029/2007JB005120.

Tamura, Y., et al. (2009), Silicic magmas in the Izu-Bonin oceanic arc and implications for crustal evolution, *J. Petrol.*, *50*(4), 685–723.

Tani, K., D. J. Dunkley, J.-I. Kimura, R. J. Wysoczanski, K. Yamada, and Y. Tatsumi (2012), Syncollisional rapid granitic magma formation in an arc-arc collision zone: Evidence from the Tanzawa plutonic complex, Japan, *Contrib. Mineral. Petrol.*, *38*(3), 215–218.

Taylor, R. N., and J. G. Mitchell (1992), K-Ar dating results from whole rock and mineral separates of the Izu-Bonin forearc basement, Leg 126, in *Proceedings of the Ocean Drilling Program, Scientific Results Leg 126*, edited by E. M. Barbu and A. P. Julson, pp. 677–680, Ocean Drill. Program, College Station, Tex.

Taylor, R. N., and R. W. Nesbitt (1995), Arc volcanism in an extensional regime at the initiation of subduction: A geochemical study of Hahajima, Bonin Islands, Japan, in *Volcanism Associated With Extension at Consuming Plate Margins, Geol. Soc. Spec. Publ.*, vol. *81*, edited by J. Smellie, Geol. Soc. of London, London, U. K.

Taylor, R. N., R. W. Nesbitt, P. Vidal, R. S. Harmon, B. Auvray, and I. W. Croudace (1994), Mineralogy, chemistry, and genesis of the boninite series volcanics, Chichijima, Bonin Islands, Japan, *J. Petrol.*, *35*(3), 577–617.

Taylor, R. N., O. Ishizuka, and C. G. Macpherson (2003), Pb isotope constraints on the source of boninite and arc magmatism in the Bonin islands, Japan, *Geochim. Cosmochim. Acta*, *67*(suppl.), A478.

Todt, W., R. A. Cliff, A. Hanser, and A. W. Hofmann (1996), Evaluation of a $^{202}Pb + ^{205}Pb$ double spike for high precision lead isotope analyses, in *Earth Processes: Reading the Isotopic Code, Geophys. Monogr. Ser.*, vol. *95*, edited by A. Basu and S. R. Hart, pp. 429–437, AGU, Washington, D. C.

Umino, S. (1985), Volcanic geology of Chichijima, the Bonin Islands (Ogasawara Islands), *J. Geol. Soc. Jpn.*, *91*, 505–523.

Weis, D., and F. A. Frey (1991), Isotope geochemistry of ninety-east Ridge basalts: Sr, Nd, Pb evidence for the involvement of the Kerguelen hot spot, in *Proceedings of the Ocean Drilling Program, Scientific Results Leg 121*, edited by E. K. Mazullo, pp. 591–610, Ocean Drill. Program, College Station, Tex.

Weis, D., and F. A. Frey (1996), Role of the Kerguelen plume in generating the eastern Indian ocean seafloor, *J. Geophys. Res.*, *101*, 13,831–13,849.

Whattam, S. A., and R. J. Stern (2011), The 'subduction initiation rule': A key for linking ophiolites, intra-oceanic forearcs, and subduction initiation, *Contrib. Mineral. Petrol.*, *162*, 1031–1045.

Zindler, A., S. R. Hart, F. A. Frey, and S. P. Jakobsson (1979), Nd and Sr isotope ratios and rare earth element abundances in Reykjanes peninsula basalts: Evidence for mantle heterogeneity beneath Iceland, *Earth Planet. Sci. Lett.*, *45*, 249–262.